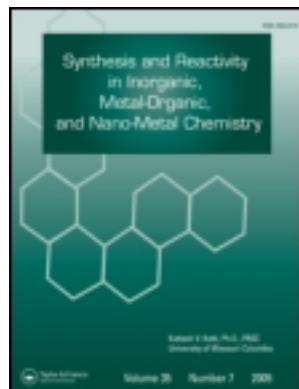


This article was downloaded by: [Iowa State University]

On: 20 August 2013, At: 14:41

Publisher: Taylor & Francis

Informa Ltd Registered in England and Wales Registered Number: 1072954 Registered office: Mortimer House, 37-41 Mortimer Street, London W1T 3JH, UK



## Synthesis and Reactivity in Inorganic, Metal-Organic, and Nano-Metal Chemistry

Publication details, including instructions for authors and subscription information:

<http://www.tandfonline.com/loi/lsrt20>

### Significantly Reduced Anisotropic Phonon Thermal Transport in Graphene Oxide Films

Wei Yu <sup>a,b</sup>, Guoqing Liu <sup>b</sup>, Jianmei Wang <sup>b,c</sup>, Xiaopeng Huang <sup>b</sup>, Huaqing Xie <sup>a</sup> & Xinwei Wang <sup>b</sup>

<sup>a</sup> School of Urban Development and Environmental Engineering, Shanghai Second Polytechnic University, Shanghai, P. R. China

<sup>b</sup> Department of Mechanical Engineering, Iowa State University, Ames, Iowa, USA

<sup>c</sup> College of Power and Mechanical Engineering, Wuhan University, Wuhan, P. R. China

Accepted author version posted online: 29 Apr 2013. Published online: 14 May 2013.

To cite this article: Wei Yu, Guoqing Liu, Jianmei Wang, Xiaopeng Huang, Huaqing Xie & Xinwei Wang (2013) Significantly Reduced Anisotropic Phonon Thermal Transport in Graphene Oxide Films, *Synthesis and Reactivity in Inorganic, Metal-Organic, and Nano-Metal Chemistry*, 43:9, 1197-1205, DOI: [10.1080/15533174.2012.756904](https://doi.org/10.1080/15533174.2012.756904)

To link to this article: <http://dx.doi.org/10.1080/15533174.2012.756904>

PLEASE SCROLL DOWN FOR ARTICLE

Taylor & Francis makes every effort to ensure the accuracy of all the information (the "Content") contained in the publications on our platform. However, Taylor & Francis, our agents, and our licensors make no representations or warranties whatsoever as to the accuracy, completeness, or suitability for any purpose of the Content. Any opinions and views expressed in this publication are the opinions and views of the authors, and are not the views of or endorsed by Taylor & Francis. The accuracy of the Content should not be relied upon and should be independently verified with primary sources of information. Taylor and Francis shall not be liable for any losses, actions, claims, proceedings, demands, costs, expenses, damages, and other liabilities whatsoever or howsoever caused arising directly or indirectly in connection with, in relation to or arising out of the use of the Content.

This article may be used for research, teaching, and private study purposes. Any substantial or systematic reproduction, redistribution, reselling, loan, sub-licensing, systematic supply, or distribution in any form to anyone is expressly forbidden. Terms & Conditions of access and use can be found at <http://www.tandfonline.com/page/terms-and-conditions>

# Significantly Reduced Anisotropic Phonon Thermal Transport in Graphene Oxide Films

Wei Yu,<sup>1,2</sup> Guoqing Liu,<sup>2</sup> Jianmei Wang,<sup>2,3</sup> Xiaopeng Huang,<sup>2</sup> Huaqing Xie,<sup>1</sup> and Xinwei Wang<sup>2</sup>

<sup>1</sup>School of Urban Development and Environmental Engineering, Shanghai Second Polytechnic University, Shanghai, P. R. China

<sup>2</sup>Department of Mechanical Engineering, Iowa State University, Ames, Iowa, USA

<sup>3</sup>College of Power and Mechanical Engineering, Wuhan University, Wuhan, P. R. China

---

Graphene oxide film has great potential applications in many fields. In this work, the flexible GO film was prepared by a assemble method under a directional flow, and the thermophysical properties of the layer film material were investigated. The results indicated the strong anisotropic thermal conductivity in GO film, and there were significantly reduced anisotropic phonon thermal transport in graphene oxide films.

---

**Keywords** anisotropic, graphene oxide film, thermal conductivity, thermal diffusivity

## INTRODUCTION

Carbon films such as diamond-like film<sup>[1]</sup> and carbon nanotube film (buckypaper)<sup>[2]</sup> have attracted much attention due to the various properties such as high electrical resistivity, high thermal conductivity, extreme hardness, chemical inertness, good optical transparency, and surface smoothness. Graphene is a monolayer of graphite in which a carbon backbone forms a two-dimensional hexagonal structure. Since its discovery, graphene has attracted much interest not only in studying its fundamental physical or chemical properties, but also in many potential applications such as field effect transistors, cellular imaging and drug delivery, ultrasensitive sensors, and supercapacitors.<sup>[3–5]</sup>

Recent experimental results showed that graphene has superior thermal conductivity. It is beneficial for electronic ap-

plications and graphene can be used as an excellent material for thermal management. Balandin et al. reported the first experimental investigation of thermal conduction of a suspended single-layer graphene obtained by micromechanical exfoliation of graphite.<sup>[6]</sup> The thermal conductivity was reported to be about 5000 W/m·K, far better than carbon nanotubes. The thermal conductivity for the monolayer graphene grown by chemical vapor deposition is about 2500 and 1400 W/m·K at room temperature and 500 K, respectively, higher than the reported values for graphite.<sup>[7]</sup> The thermal transport in few-layer graphene shows that the room temperature thermal conductivity changes from ~2800 to ~1300 W/m·K as the number of atomic planes varies from 2 to 4.<sup>[8]</sup> Based on the micro-Raman scattering technique, Faugeras et al. obtained the 3D equivalent thermal coefficient of graphene at about 630 W/m·K, still validating that graphene was a very good thermal conductor.<sup>[9]</sup> For suspended thermally reduced graphene oxide (GO) flakes, the thermal conductivity determined by an electrical method is in the range of 0.14–2.87 W/m·K.<sup>[10]</sup>

GO film (paper) is a new kind of layered material.<sup>[11]</sup> It outperforms many other paper-like materials in stiffness and strength, combining the macroscopic flexibility and stiffness of a unique interlocking-tile arrangement of the nanoscale GO sheets. It was found that suspended GO-based membranes not only exhibited a high Young's modulus but also showed quality factors comparable to diamond resonators.<sup>[12]</sup> In addition, GO film has great potential applications in field effect transistors,<sup>[13]</sup> nanomechanical devices,<sup>[14]</sup> batteries, supercapacitors, electronic and optoelectronic components, and molecular storage. Up to now, a lot of work has been done on the thermal properties of graphene, while most work focused on the thermophysical properties of single-layer or few-layer graphene, little knowledge is available for the thermal transport in GO films, whose preparation can be readily scaled up and have great potential applications. The functional groups in GO films and interlocking structure are expected to significantly enhance phonon scattering and reduce the thermal transport significantly.

---

Received 19 November 2012; accepted 4 December 2012.

The work was supported by National Natural Science Foundation of China (51106093 & 51176106), Program for New Century Excellent Talents in University (NECT-10-883), the Basic Research Foundation of Shanghai Science and Technology Committee (12JC1404300), and Program for Professor of Special Appointment (Eastern Scholar) at Shanghai Institutions of Higher Learning.

Address correspondence to Huaqing Xie, School of Urban Development and Environmental Engineering, Shanghai Second Polytechnic University, Shanghai 201209, P. R. China. E-mail: hqxie@eed.sspu.cn

This study reported on the significantly reduced anisotropic phonon thermal transport in GO films. In this study, the in-plane thermal diffusivity and conductivity measurement for GO film were performed by a transient electrothermal (TET) technique. A pulsed laser-assisted thermal relaxation (PLTR) technique was used to verify the data obtained by TET technique. A modified laser flash method was developed to measure the cross-plane thermal diffusivity of GO films. These technologies provide full capacity measurement of the thermal conductivity and diffusivity of GO films in the in-plane and cross-plane directions and enable first-time study of the relation among these properties.

## EXPERIMENTAL

### Preparation and Structure Analysis of GO Films

The flexible GO film was prepared by the assembly method under a directional flow.<sup>[11]</sup> In a typical preparation process, graphite oxide should be synthesized from expandable graphite (NYACOL Nano Technologies Inc., Ashland, MA, USA) by the Hummers method.<sup>[15]</sup> Graphite oxide can undergo complete exfoliation in water with the aid of ultrasound (Fisher Scientific, Pittsburgh, PA, USA, FS60H ultrasonic cleaning bath), and it will yield colloidal suspensions of almost entirely individual GO sheets. GO films are made by filtration of the resulting colloid through an anodisc membrane filter (47 mm in diameter, 0.2  $\mu\text{m}$  pore size; Whatman filter paper). GO sheets can be assembled into well-ordered macroscopic structures under a directional flow. After drying, free-standing GO paper can be peeled from the filter. The GO paper was dried at 50°C in vacuum ( $<10^{-3}$  Torr) for half an hour. The layer-to-layer distance was measured using X-ray diffraction, and measurement was carried out with a Siemens D 500 diffractometer (New York, NY, USA) (Cu Ka radiation, operating at 45 keV, cathode current of 30 mA, 0.15 detector slits) using the specular reflection mode. Raman spectra were taken with Voyage confocal Raman spectrometer (Newark, DE, USA) with 532 nm wavelength incident laser light.

### The In-Plane Thermophysical Properties Characterization for GO Films

The TET technique is a rapid and convenient method to measure the thermophysical properties of conductive, semiconductive, and nonconductive materials with strong signal level. A schematic of the TET experiment setup is shown in reference.<sup>[15]</sup> The to-be-measured sample serves as a heater and a temperature sensor simultaneously. The GO film is nonconductive, so the surface of GO film should be coated with a thin Au film. At the beginning of the experiment, a step direct current is fed through the film to introduce electrical heating. The transient temperature rise is small, so the radiation effect is negligible for our measurement. Therefore, the governing equation of this one-dimensional heat conduction problem can be simplified as

$$\frac{\partial(\rho c_p T)}{\partial t} = k \frac{\partial^2 T}{\partial x^2} + q_0. \quad [1]$$

Where  $r$ ,  $c_p$ , and  $k$  are density, specific heat, and thermal conductivity of the sample, respectively.  $q_0$  is the electric heating power. Detailed procedure to solve this governing equation is given in Guo's work.<sup>[16]</sup> The average temperature of the sample  $T(t)$  is calculated as

$$T(t) = \frac{1}{L} \int_{x=0}^L T(x, t) dx = T_0 + \frac{8q_0 L^2}{k\pi^4} \sum_{m=1}^{\infty} \frac{1 - \exp[-(2m-1)^2 \pi^2 \alpha t / L^2]}{(2m-1)^4}. \quad [2]$$

Therefore, the normalized temperature increase,  $T^*(t) = [T(t) - T_0] / [T(t \rightarrow \infty) - T_0]$ , can be written as

$$T^* = \frac{96}{\pi^4} \sum_{m=1}^{\infty} \frac{1 - \exp[-(2m-1)^2 \pi^2 \alpha t / L^2]}{(2m-1)^4}. \quad [3]$$

When the temperature change is not large, it is physically reasonable to assume that the resistance change of the Au coating has a linear relationship with its average temperature change. Therefore, the measured  $\Delta V \sim t$  ( $V$ , voltage;  $t$ , time) shares the same shape as the  $\Delta T \sim t$  curve. The shape of the normalized  $\Delta V \sim t$  curve can be used to determine the thermal diffusivity of the sample. The influence of Au film on heat transfer can be subtracted by using the Lorenz number ( $L_{Lorenz}$ ) without increasing the uncertainty.<sup>[16]</sup>

$$\alpha = \alpha_e - \frac{L_{Lorenz} T L}{R A \rho c_p}, \quad [4]$$

where  $\alpha_e$  is the thermal diffusivity directly determined from the normalized  $DV \sim t$  curve, and  $a$  is the real thermal diffusivity of the GO film. From Eq. (2), it is concluded that when the step DC current time fed through the film goes to infinity, the temperature distribution along the sample will reach the steady state, and the average temperature of the sample is

$$T(t \rightarrow \infty) = T_0 + q_0 L^2 / (12k). \quad [5]$$

Therefore, the temperature rise from the initial temperature to the steady state is  $\Delta T = T(t \rightarrow \infty) - T_0 = q_0 L^2 / (12k)$ .  $q_0$  is the electrical heating power per unit volume and can be expressed as  $q_0 = I^2 R / (AL)$ , while the  $A$  and  $L$  are the cross-sectional area and length of the sample, respectively. The thermal conductivity  $k$  can be determined as

$$k = I^2 R L / (12A \Delta T). \quad [6]$$

In the experiment, the temperature rise can be evaluated from the resistance change of the sample ( $DR$ ) as  $\Delta T = \Delta R / \eta = \Delta V / I \eta$ .  $t_{\perp} \eta$  is the temperature coefficient of resistance of the sample and can be obtained in a separate calibration experiment by measuring the electrical resistance of the sample at different temperatures. The current is constant, and voltage change of the

sample will be monitored by using an oscilloscope. It is clear that when the temperature coefficient of resistance ( $dR/dT$ ) is calculated, the thermal conductivity can be obtained.

The Au-coated GO film is free suspended between two aluminum electrodes by silver paste. A  $K$ -type thermocouple is attached to one side of the electrode, close enough to the sample, and the other end of the thermocouple is connected to a thermocouple meter to simultaneously monitor the temperature change. In the calibration process, the sample was heated externally (not electrically). The whole stage, including the aluminum electrodes and the sample suspended between the electrodes, is positioned on a heating plate in a vacuum chamber whose pressure is lower than  $10^{-3}$  Torr to reduce unnecessary heat dissipation. The stage was heated, and then it would be slowly cooled down. Due to the surrounding vacuum atmosphere, the cooling process is very slow, the time can be assumed to be long enough to achieve even temperature distribution and the readings from the thermocouple meter can be used as the temperature of the sample. Temperature and resistance readings are recorded to attain the temperature-resistance calibration profile for further data processing. Details of experimental conditions and results for GO film characterized by using TET technique is shown in Table 1.<sup>[17]</sup>

The real thermal conductivity of the GO film can be obtained through subtracting the effect of the Au film as  $k = k_e - L_{Lorenz}TL/(RA_w)$ . In order to verify the reliability of the thermal diffusivity obtained from TET technique, the PLTR technique is also applied to measure the thermal diffusivity along the in-plane direction of GO films. PLTR is a method developed in our group to measure the thermal diffusivity of the specimen along the in-plane direction. In this experiment, the front surface of the specimen, which is coated with 40-nm-thick Au film, is uniformly irradiated by a nanosecond laser pulse. A temperature rise occurs in the front surface and heat transfer begins along the cross-plane direction and in-plane direction. Giving enough time, the heat transfer along the cross-plane direction will make the sample have uniform temperature in the cross-section, and the long-term heat transfer is controlled by that in the lateral (length direction). A small dc is fed through the sample to detect the resistance change for that it has a linear relationship with the temperature change. The normalized temperature relaxation can be written as<sup>[18]</sup>

$$T^* = \frac{8L^2}{\alpha \Delta t \pi^4} \sum_{m=1}^{\infty} \frac{\exp[-(2m-1)^2 \pi^2 \alpha t / L^2] \{ \exp[(2m-1)^2 \pi^2 \alpha \Delta t / L^2] - 1 \}}{(2m-1)^4} \quad [7]$$

where  $T^*$  is the normalized average temperature change in the specimen,  $\alpha$  is the thermal diffusivity along the lateral direction,  $L$  is the specimen length, and  $\Delta t$  is the laser pulse width.

TABLE 1  
Details of experimental conditions and results for GO film characterized by using TET technique<sup>[17]</sup>

Sample	1	2
Length (mm)	1.98	2.59
Width (mm)	0.673	0.471
Thickness (mm)	0.054	0.076
Initial resistance ( $\Omega$ )	49.898	522.200
Final resistance ( $\Omega$ )	50.657	502.306
Temperature change (K)	14.88	28.86
DC current (mA)	12	4
Effective thermal diffusivity ( $\times 10^{-6}$ m <sup>2</sup> /s)	1.46	1.57
Real thermal diffusivity ( $\times 10^{-6}$ m <sup>2</sup> /s)	1.45	1.57
Effective thermal conductivity (W/m·K)	2.22	1.69
Real thermal conductivity (W/m·K)	2.21	1.68

Since Au is an excellent conductor for heat transfer, the coated Au film will have some effect on the measured thermal diffusivity, especially for thin specimens. This kind of effect can be ruled out by using the concept of thermal conductance. Derivations and explanations of this method are detailed in work by Guo et al.<sup>[16]</sup>

There are two methods to determine the thermal diffusivity of the specimen. One is based on a characteristic point on the temperature relaxation curve. The other one is based on global data fitting of the temperature. The latter one is used in our experiment. Table 2 contains all the detailed experiment parameters and results.

### Out-of-Plane Thermal Diffusivity Measurement for GO Films

The flash technique has been widely used for the measurement of thermal diffusivity. In the experiment, a short energy pulse (flash light or laser) is used to uniformly irradiate the front surface of the specimen. A temperature rise occurs in the front surface and heat transfer begins along the out-of-plane direction. Typically, a set of preamplifier and infrared detector is used to detect temperature response signal of the rear surface.

TABLE 2  
Details of experimental conditions and results for PLTR technique

	Data
Length (mm)	2.26
Width (mm)	0.717
Thickness (mm)	0.077
Resistance of the sample ( $\Omega$ )	65
DC current (mA)	3
Effective thermal diffusivity ( $\times 10^{-6}$ m <sup>2</sup> /s)	1.35
Real thermal diffusivity ( $\times 10^{-6}$ m <sup>2</sup> /s)	1.32

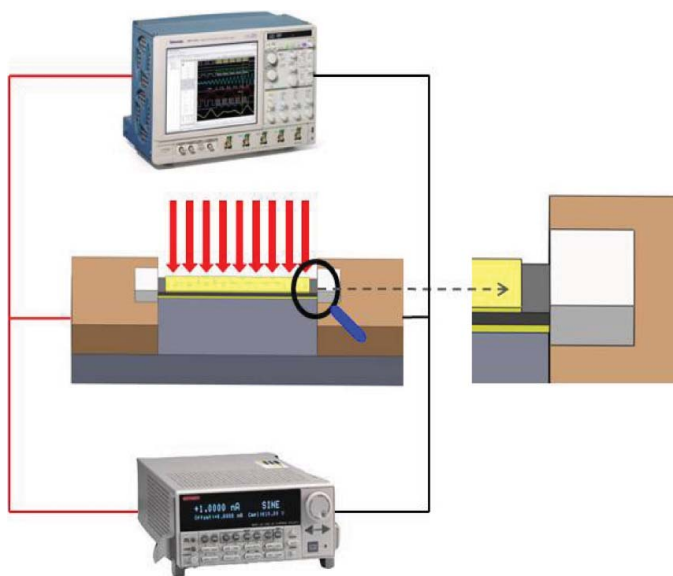


FIG. 1. Block diagrams of the experimental system for the modified laser flash technique for cross-plane thermal diffusivity measurement of GO films (color figure available online).

But sometimes, the specimen is too small and it is difficult to collect the signal. In this work, a modified laser flash technique is developed for very small sample measurement.

In the experiment, the specimen GO film is coated with 40-nm-thick Au film on one side and then suspended over two copper electrodes as shown in Figure 1. The coated side, which acts as the rear surface, is placed downward on the electrodes. Silver paste is placed at the specimen/electrode contacts to enhance the thermal and electrical connection. In order to make sure that the energy of the laser pulse is totally absorbed by the front surface of the specimen, the front surface is coated with 100-nm-thick Au film. But this Au film is not connected in the circuit. To do this, during the coating process, two small glass pieces are put near the wire/electrode contacts as shelter. Figure 1 shows the setup of the experiment.

For Au coating on the backside of GO, if the temperature change is not large, it is physically reasonable to assume that its resistance change has a linear relationship with its average temperature change. During the experiment, a small constant dc is fed through the specimen to detect the temperature change for the reason that the temperature change will correspondingly lead to a resistance change. As a result, there will be a voltage change ( $\Delta V$ ) over the specimen. Therefore, the measured  $\Delta V \sim t$  ( $t$ , time) shares the same shape as the  $\Delta T \sim t$  curve. The shape of the normalized  $\Delta V \sim t$  curve can be used to determine the thermal diffusivity of the specimen. In the experiment, the top surface of the sample is irradiated with a nanosecond laser pulse whose pulse duration is 5–8 ns, with a pulse energy about 225 mJ and a spot size of 7 mm. The experiment is conducted in a vacuum chamber and the pressure level is  $1 \times 10^{-3}$  Torr.

The half-rise time method to derive the thermal diffusivity is expressed as<sup>[19]</sup>

$$\alpha = (1.38L^2/\pi^2t_{1/2}) \quad [8]$$

where  $\alpha$  is the thermal diffusivity of the specimen,  $L$  is the specimen thickness, and  $t_{1/2}$  is the half-rise time which is required for the rear-surface temperature to reach one half of the maximum temperature rise. This equation means that the thermal diffusivity is determined by measurements of length, time, and temperature.

## RESULTS AND DISCUSSION

### Structure of GO Films

The free-standing GO membrane material with the layered structure was made by flow-directed assembly method. X-ray diffraction (XRD) pattern analysis (Figure 2) shows that the 002 reflection of graphite at  $2\theta = 26.21^\circ$  almost completely disappears. It indicates that the interlayer space of graphite becomes mostly intercalated by oxygen-containing functional groups upon oxidation. The layering in the GO paper is evident from its XRD pattern. The GO paper exhibits a characteristic peak at  $12.07^\circ$   $2\theta$  corresponding to the 002 interplanar spacing of 0.7334 nm, which is the layer-to-layer distance ( $d$ -spacing). The  $d$ -spacing depends strongly on the water content. Interlayer distance from 0.55 (anhydrous) nm to 0.86 nm (about 43 wt% of water) has also been observed in other research.<sup>[20]</sup> Therefore for the prepared GO paper, there are some absorbed water molecules due to the strong hydrogen-bonded interaction between the GO sheets and water molecules.

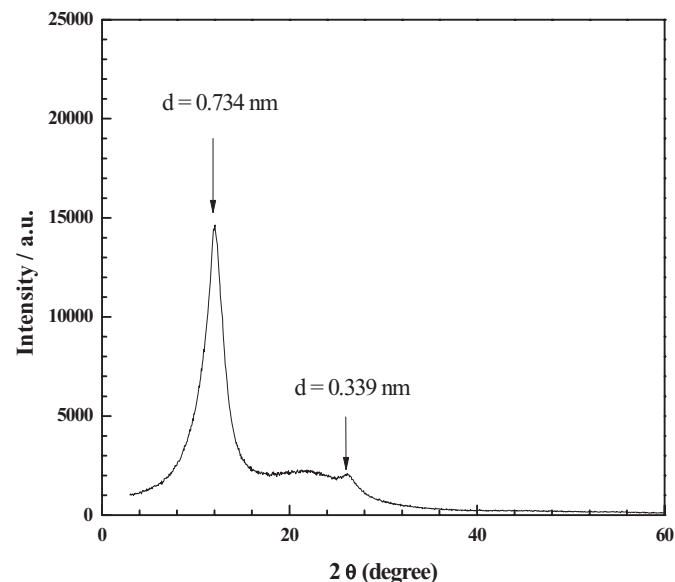


FIG. 2. X-ray diffraction pattern for the prepared GO film.

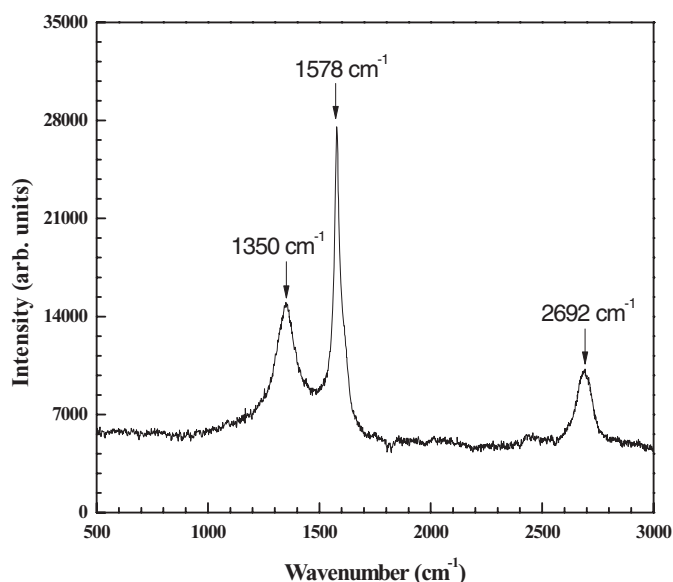


FIG. 3. The Raman spectrum of GO film.

Raman spectrum of the GO film is shown in Figure 3, showing the two typical bands observed in carbon materials: the D band at  $1350\text{ cm}^{-1}$  and the G band at  $1578\text{ cm}^{-1}$ . The G band corresponds to the first-order scattering of the  $E_{2g}$  in-plane deformation vibrations in the graphene layers. The D peak is from the structural imperfections created by the attachment of hydroxyl and epoxide groups on the carbon basal plane. The defects can be related to several features: the presence of edges in small crystals, deviations from planarity, and the presence of a certain number of C atoms in the  $sp^3$  hybridization state, etc.<sup>[20]</sup>

GO is a hydrophilic oxygenated graphene sheets. GO sheets can be reassembled to be the layer GO film bearing oxygen functional groups on their basal planes and edges. The most accepted structure of GO is that epoxy and hydroxyl groups decorate the surface of carbon sheets and the carboxyl groups are localized at the edges.<sup>[21,22]</sup> Figure 4 demonstrates the structure of GO films. The GO film is highly anisotropic, which could be reflected by its thermophysical properties.

### Thermal Transport Along the In-Plane Direction of GO Films

The thermal diffusivity along the in-plane direction ( $\alpha_{||}$ ) of GO films was measured by using the TET technique. The microscopic images of the samples are shown in Figure 5. By measuring evolution of the voltage over the sample, the temperature evolution of the sample can be sensed. Consequently, the thermal diffusivity of the sample can be obtained by fitting the temperature change curve against time. Our previous experiments proved that the Au film on the nonconductive material needs to be as thin as possible in order to obtain high accuracy in measuring the thermal diffusivity.<sup>[16]</sup> In this work, we tried to control the thickness of Au film on the two samples about 20 nm,

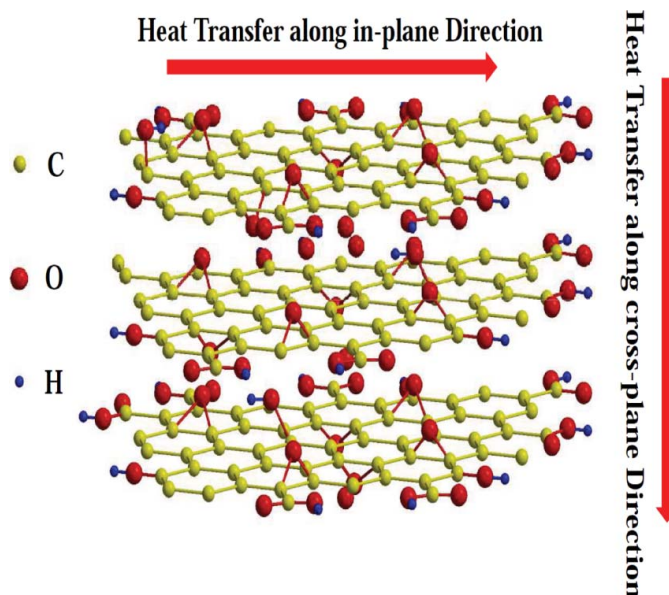


FIG. 4. Schematic structure of the layered GO film and the heat transfer along in-plane and out-of-plane directions (color figure available online).

but the electrical resistances vary much due to the difficulty in controlling so thin Au film. So sample 1 with low electrical resistance shows positive temperature coefficient of resistance like metal, while the temperature coefficient of resistance is negative for sample 2 with high electrical resistance maybe due to the discontinuous Au film on the surface of sample. In order to reduce the radiation heat loss from the film surface, the temperature change should be small. Therefore, smaller DC current is better as long as necessary signal level can be satisfied. When conducting experiments, the DC current for low resistance sample 1 is 12 mA, while for the sample 2 with high resistance, the current is 4 mA, and the temperature rise of the latter is much larger than that of the former. The temperature rises of the two samples are both no more than  $30^\circ\text{C}$ , so the radiation heat loss is negligible. It should be noted that in addition to the

TABLE 3

Details of experimental conditions and results for modified flash method technique

	Data 1	Data 2	Data 3
Length (mm)		3.68	
Thickness (mm)		0.053	
Resistance of the sample ( $\Omega$ )		120	
DC current (mA)		3	
Thermal diffusivity by half-rise time method ( $\times 10^{-7}\text{ m}^2/\text{s}$ )	1.74	1.68	1.62
Average thermal diffusivity ( $\times 10^{-7}\text{ m}^2/\text{s}$ )		$1.68 \pm 0.05$	



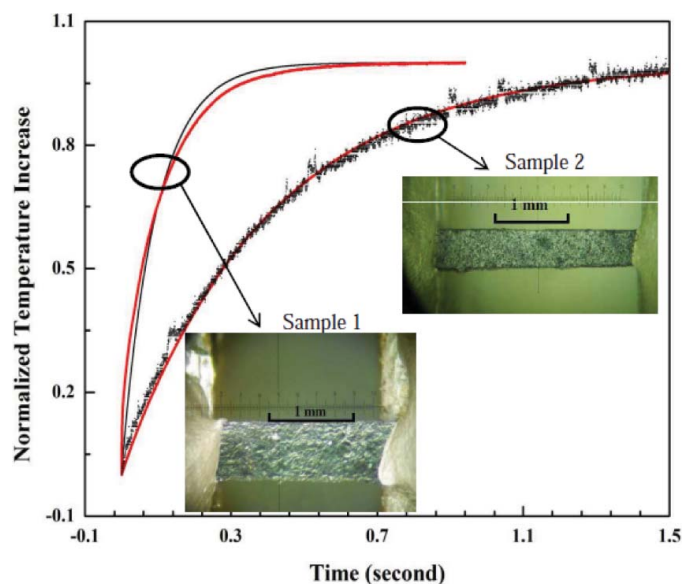


FIG. 5. Normalized temperature increase versus the fitting results for the GO film along in-plane direction, measured by TET experiments. The solid red lines are the theoretical values for each sample. The black dots are the experimental data measured. The insets are the sample pictures under microscope (color figure available online).

measurement accuracy, the large temperature rise will influence the structure of GO film, because the structure of GO film is sensitive to the temperature. GO films will burn out under high temperatures.

Least square fitting method was employed to find the thermal diffusivity. In this method, the normalized temperature increase is calculated using Eq. 3 by using different trial values of the thermal diffusivity. The trial value giving the best fit (least square) of the experimental data is taken as the sample's property. Figure 5 illustrates the normalized temperature increase versus the fitting results for the GO films along the in-plane direction. The thermal diffusivities of sample 1 and sample 2 are  $1.46 \times 10^{-6}$  and  $1.57 \times 10^{-6} \text{ m}^2/\text{s}$ , respectively. The difference maybe comes from the tiny structure difference of the samples, such as the density, and the content of water in the GO film. What we obtained now is the effective thermal diffusivity ( $\alpha_e$ ) that includes the effect of the Au coating. As discussed in the In-Plane Thermophysical Properties Characterization for GO Films section, there is a thin Au film coated on the film, so the effect of Au coating should be ruled out using the concept of thermal conductance as indicated in Eq. 4. In Eq. 4,  $Cp(\rho \times c_p)$  should be known first to rule out the effect of the Au coating. Here we estimated the value of  $Cp$  using the ratio of effective thermal conductivity ( $k_e$ ) and effective thermal diffusivity ( $\alpha_e$ ). As shown in Table 1, the obtained real thermal diffusivity is very close to the effective thermal diffusivity. This is because the thickness of Au film is thin compared with the thickness of GO film, and the thermal conductivity of Au film is much smaller than the bulk material value. Therefore in this work the thin Au film has very limited

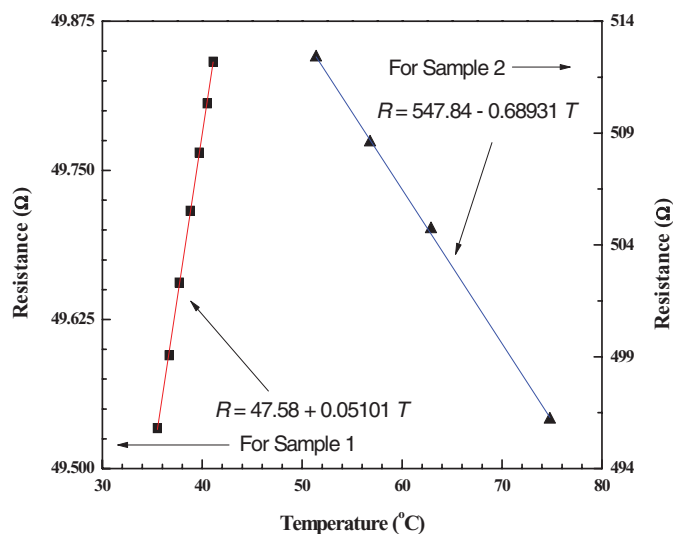


FIG. 6. Linear fitting curve of temperature coefficient of resistance for the GO films, measured by TET experiments (color figure available online).

effect on the heat transfer along the in-plane direction in the GO film.

The thermal conductivity of the sample can be obtained using Eq. 6. The calibration data for electrical resistance against temperature is displayed in Figure 6. A linear relationship is fitted to obtain the temperature coefficient of resistance. The obtained calibration profile for sample 1 with smaller resistance presents a temperature-resistance property similar to a good conductor, while sample 2 with larger resistance shows a negative resistance temperature coefficient (e.g., graphite). The temperature coefficients of resistance for sample 1 and sample 2 are 0.051 and  $-0.689 \text{ } \Omega/\text{K}$ , respectively. Figure 7 shows the measured voltage change versus time. The obtained effective thermal conductivity for sample 1 and sample 2 is 2.22 and 1.69 W/m-K, respectively. After subtracting the effect of the Au coating, the real thermal conductivity for samples 1 and 2 is 2.21 and 1.68 W/m-K, respectively.

The PLTR technique was also used to measure the thermophysical properties along the in-plane direction of GO films. The outcome is shown in Table 2 and Figure 8. The measured thermal diffusivity is  $1.32 \times 10^{-6} \text{ m}^2/\text{s}$ , smaller than those obtained from TET technique, but in the same order of magnitude. The difference maybe comes from the different structure of GO film sample. The structure of GO film is very sensitive to the preparation condition and surrounding circumstances. The content of absorbed water in GO film may vary greatly with the slight change of circumstance, and it will greatly affect its thermophysical properties. What is certain is that there is a significantly reduced thermal transport in GO film comparing with single-layer graphene.

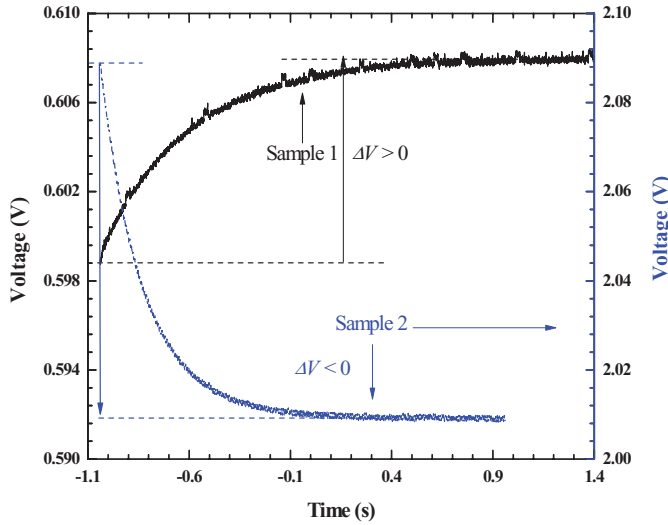


FIG. 7. The measured voltage change versus time.  $\Delta V = V_1 - V_0$  can be used to determine  $\Delta R$  and  $\Delta T$ , and then determine the thermal conductivity (color figure available online).

### Thermal Transport Along the Cross-Plane Direction of GO Films

A modified laser flash technique is developed to measure the thermal diffusivity along the cross-plane direction. We have done the experiments for three times. Figure 9 shows the sample signal and reference signal of heat transfer along the cross-plane direction. Table 3 contains all the detailed experiment parameters and results. It was mentioned previously that a temperature rise occurs in the front surface and heat transfer begins along the cross-plane direction of the sample after laser irradiation. In fact, the heat transfer occurs through two directions of the sample at the same time. One is along the cross-plane direction and the other along the in-plane direction. From Figure 9, it is seen that it takes less than 20 ms for the temperature of rear surface to reach the peak. In the following 30 ms, the curve of the signal keeps horizontal and does not show any sign of drop.

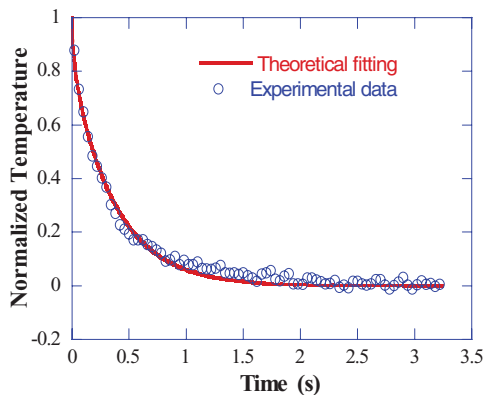


FIG. 8. The normalized temperature versus the theoretical fitting (color figure available online).

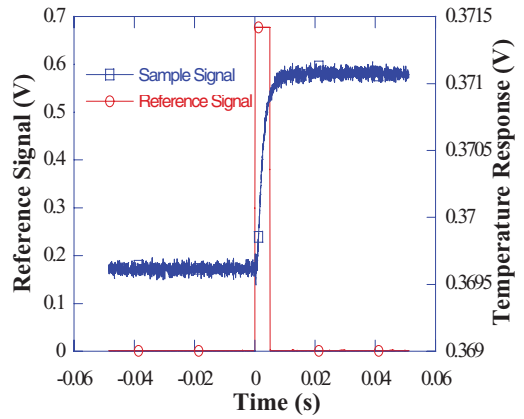


FIG. 9. Heat transfer along the cross-plane direction (color figure available online).

From Figure 10, it is obvious that to complete the whole process of heat transfer along the in-plane direction, it will take about several seconds. From the angle of characteristic heat transfer length, it is also easy to prove that in the very beginning, heat transfer along the in-plane direction will not affect that along the cross-plane direction  $L_c = (a_{\parallel t})^{1/2}$ , where  $L_c$  stands for characteristic heat transfer length along the in-plane direction,  $\alpha_{\parallel}$  is the thermal diffusivity along the in-plane direction, and  $t_{\perp}$  is full-rise time, which is required for the rear-surface temperature to reach the maximum temperature rise. The value of  $\alpha_{\parallel}$  is  $1.32 \times 10^{-6} m^2 s^{-1}$  and  $t_{\perp}$  is less than 0.02 second. So  $L_c$  is about 0.162 mm. when it is divided by the value of specimen length, the ratio turns out to be 0.0442. It is reasonably negligible. As a result, the heat transfer loss in the in-plane direction is negligible in this modified laser flash technique and our method is reliable to determine the thermal diffusivity along the cross-plane direction.

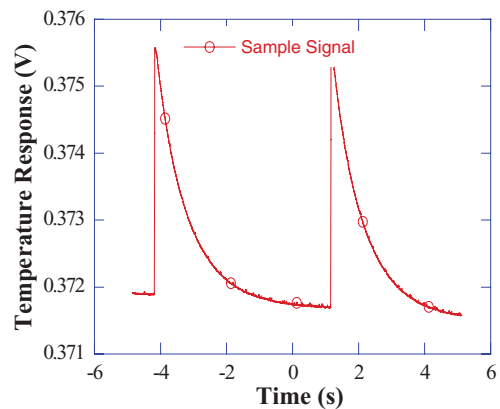


FIG. 10. Profile of the back surface temperature evolution along the in-plane direction (color figure available online).



## Anisotropic Thermal Transport and the Factors Influencing the Heat Transport in GO Film

The previous results indicate the strong anisotropic thermal conductivity in GO film. The thermal transport along cross-plane direction is about one order of magnitude below that along in-plane direction. The heat transfer anisotropy reflects the anisotropy for the structure of GO film, which was discussed in the Structure of GO Films section. In the TET experiment, the characteristic time ( $t_1$ ) of heat transfer along in-plane direction of GO film is about 2s ( $\sim l^2/\alpha_{\parallel}$ :  $l$ , length of the sample;  $\alpha_{\parallel}$ , effective thermal diffusivity along the in-plane direction). On the other hand, along the sample cross-plane direction, the characteristic heat transfer time ( $t_2$ ) is about  $10^{-2}$  s ( $\sim d^2/\alpha_{\perp}$ :  $d$ , thickness of the sample;  $\alpha_{\perp}$ , effective thermal diffusivity along the cross-plane direction). Therefore during the TET experiment, the heat transfer in the cross-sectional direction of the sample is significantly faster than that in the length direction, which makes it safe to assume the sample has uniform temperature distribution in its cross-section. It is physically reasonable to assume that the heat transfer is one-dimensional along the length direction of the sample. The conclusion is similar to that of the outcome in the modified laser flash technique. The relative contribution of the electron and phonon components to the thermal conductivity can be evaluated on the basis of the Lorenz number,  $L_{Lorenz} = k/\sigma T$ , where  $L_{Lorenz}$  and  $\sigma$  are the Lorenz number and the electrical conductivity. The electrical conductivity of GO film has been investigated before, it is about  $0.408 \text{ Sm}^{-1}$ ,<sup>[23]</sup> therefore the Lorenz number at room temperature for GO film is  $0.016 \text{ W}/\Omega \text{ K}^2$ . The Lorenz number is very large, corresponds to a ratio of the electron to phonon contribution to the thermal conductivity of 1 to  $10^6$ , therefore phonon play the major role to the thermal transport, and the contribution of electron to the thermal conductivity of GO film is negligible.

Up to now, there is no thermal conductivity data about GO film, so the thermal properties of other carbon materials serve as a benchmark for the results reported herein. Shamsa et al. reported the thermal conductivity of a variety of carbon films ranging from polymeric hydrogenated amorphous carbon to tetrahedram amorphous carbon.<sup>[24]</sup> The thermal conductivity of diamond-like carbon films mainly constituted by  $sp^3$  C-C bonds is in a comparable range to the GO film of the present study. GO film consists of a hexagonal ring-based carbon network having both  $sp^2$ -hybridized carbon atoms and  $sp^3$ -hybridized carbons bearing hydroxyl and epoxide functional groups on either side of the sheet. So the bond types of GO and tetrahedram amorphous carbon are similar, and it is reasonable that their thermal conductivities are close. The extensive presence of saturated  $sp^3$  bonds and oxygen atoms makes GO film nonconducting, and hinders the thermal transport and promotes phonon scattering effects. Schwamb et al. used an electrical method to measure the thermal conductivity of reduced GO nanostructures.<sup>[10]</sup> They found the thermal conductivities of reduced GO are in the range of 0.14–2.87 W/m·K. It should be noted that the property of graphene is influenced greatly by the preparing process, and its

electrical conductivity is tunable in a large range.<sup>[25]</sup> Therefore the large thermal conductivity deviation among experiments by different groups is reasonable, and it strongly depends on the synthesis method.

As is known, pristine graphene has a markedly higher thermal conductivity by a factor of  $10^3$  W/m·K, so it is an interesting issue to investigate the factors influencing the heat transport in GO film. The thermal conductivity is one of the important macroscopic physics properties, and it reflects the microscopic structure in essence. In our opinion, the following two factors may have great influence on the thermal transport in GO film. First, the thermal contact resistance between the adjacent GO is not ignored. In our previous work,<sup>[26]</sup> it is found that the size of GO is in the range of 0.5–3  $\mu\text{m}$ , therefore the millimeter-sized GO film is stacked together and bridged by thousands of GO nanosheet, and the total thermal contact resistance may be large enough to influence the heat transport along in-plane direction greatly. Xie et al. measured the thermophysical properties of multiwalled carbon nanotube arrays.<sup>[2]</sup> The room temperature thermal diffusivity for the tested sample is about  $4.6 \text{ cm}^2 \text{ s}^{-1}$ , much greater than that of copper. The carbon nanotube array showed higher magnification, because there was no thermal contact resistance along axis direction, showing the excellent thermal transport properties. Second, the thermal conductivity of GO may be far below that of graphene. The oxidized chemical structure introduced lattice defects that hinder thermal transport and promote diffusion effect. As discussed previously, phonon is the main contribution to the thermal transport, so the thermal conductivity are related by  $k = Cv/l/3$ , where  $C$ ,  $v$  and  $l$  are the specific heat, the phonon wave velocity and the mean free path, respectively. It is calculated that the mean free path at room temperature is only about 0.2 nm, far below that of single-layer graphene. Our previous study illustrated that when graphite is oxidized, some of  $sp^2$ -bonded carbon atoms become  $sp^3$ -bonded atoms,<sup>[26]</sup> and about 17% of the carbon atoms in the sample were oxygenated. The oxygen atom on the surface or edge of GO will reduce the phonon mean free path greatly.

## CONCLUSIONS

In this work, the flexible GO film was prepared by a assemble method under a directional flow. The thermophysical properties of the layer film material were investigated. Suitable measurement techniques were selected to characterize the in-plane and cross-plane thermal diffusivity and conductivity. The transient electrothermal technique was used to measure the thermal conductivity along in-plane direction of GO film, and the experimental outcome was verified by PLTR technique. The real thermal conductivity along in-plane direction is 1.68–2.21 W/m·K, and the real thermal diffusivity is  $1.32\text{--}1.57 \times 10^{-6} \text{ m}^2/\text{s}$ . A modified laser flash technique is developed for the thermal conductivity measurement along cross-plane direction. The real thermal diffusivity along cross-plane direction is only  $1.68 \times 10^{-7} \text{ m}^2/\text{s}$ , about one order of magnitude below that along in-plane

direction, illustrating the strong anisotropic. It reflects the microscopic layer structure in essence. The following two factors may have great influence on the thermal transport in GO film. One is the thermal contact resistance between the adjacent GO, another is the low thermal conductivity for GO, which is caused by the lattice defects, it will hinder thermal transport and promote diffusion effect.

## REFERENCES

1. Balandin, A. A.; Shamsa, M.; Liu, W. L.; Casiraghi, C.; Ferrari, A. C. *Appl. Phys. Lett.* **2008**, *93*, 043115.
2. Xie, H.; Cai, A.; Wang, X. *Phys. Lett. A* **2007**, *369*, 120.
3. Geim, A. K. *Science* **2009**, *324*, 1530.
4. Geim, A. K.; Novoselov, K. S. *Nat. Mater.* **2007**, *6*, 183.
5. Allen, M.J.; Tung, V. C.; Kaner, R. B. *Chem Rev.* **2010**, *110*, 132.
6. Balandin, A. A.; Ghosh, S.; Bao, W.; Calizo, I.; Teweldebrhan, D.; Miao, F.; Lau, C. N. *Nano Lett.* **2008**, *8*, 902.
7. Cai, W.; Moore, A. L.; Zhu, Y.; Li, X.; Chen, S.; Shi, L.; Ruoff, R. S. *Nano Lett.* **2010**, *10*, 1645.
8. Ghosh, S.; Bao, W.; Nika, D. L.; Subrina, S.; Pokatilov, E. P.; Lau, C. N.; Balandin, A. A. *Nat. Mater.* **2010**, *9*, 555.
9. Faugeras, C.; Faugeras, B.; Orlita, M.; Potemski, M.; Nair, R. R.; Geim, A. K. *ACS Nano* **2010**, *4*, 1889.
10. Schwamb, T.; Burg, B. R.; Schirmer, N. C.; Poulidakos, D. *Nano Technol.* **2009**, *20*, 405704.
11. Dikin, D. A.; Stankovich, S.; Zimney, E. J.; Piner, R. D.; Dommett, G. H.; Evmenenko, G.; Nguyen, S. T.; Ruoff, R. S. *Nature* **2007**, *448*, 457.
12. Robinson, J. T.; Perkins, F. K.; Snow, E. S.; Wei, Z.; Sheehan, P. E. *Nano Lett.* **2008**, *8*, 3137.
13. Jin, M.; Jeong, H.; Yu, W. J.; Bae, D. J.; Kang, B. R.; Lee, Y. H. *J. Phys. D: Appl. Phys.* **2009**, *42*, 135109.
14. Robinson, J. T.; Zalalutdinov, M.; Baldwin, J. W.; Snow, E. S.; Wei, Z.; Sheehan, P.; Houston, B. H. *Nano Lett.* **2008**, *8*, 3441.
15. Compton, O. C.; Nguyen, S. T. *Small* **2010**, *6*, 711.
16. Guo, J.; Wang, X.; Wang, T. *J. Appl. Phys.* **2007**, *101*, 063537.
17. Yu, W.; Xie, H. Q.; Wang, X. W. *J. Eng. Thermophys.* **2012**, *33*, 1609.
18. Guo, J.; Wang, X.; Geohegan, D.; Eres, G.; Vincent, C. *J. Appl. Phys.* **2008**, *103*, 113505.
19. Parker, W. J.; Jenkins, R. J.; Butler, C. P.; Abbott, G. L. *J. Appl. Phys.* **1961**, *32*, 1679.
20. Barroso-Bujans, F.; Cerveny, S.; Alegría, A.; Colmenero, J. *Carbon* **2010**, *48*, 3277.
21. He, H.; Riedl, T.; Lerf, A.; Klinowski, J. *J. Phys. Chem.* **1996**, *100*, 19954.
22. Lerf, A.; He, H.; Forster, M.; Klinowski, J. *J. Phys. Chem. B* **1998**, *102*, 4477.
23. Gao, W.; Alemany, L. B.; Ci, L.; Ajayan, P. M. *Nat Chem.* **2009**, *1*, 403.
24. Shamsa, M.; Liu, W. L.; Balandin, A. A.; Casiraghi, C.; Milne, W. I.; Ferrari, A. C. *Appl. Phys. Lett.* **2006**, *89*, 161921.
25. Jung, I.; Dikin, D. A.; Piner, R. D.; Ruoff, R. S. *Nano Lett.* **2008**, *8*, 4283.
26. Yu, W.; Xie, H.; Chen, W. *J. Appl. Phys.* **2010**, *107*, 094317.